Scientific Research Publishing

Open Journal of Fluid Dynamics, 2023, 13, 1-15
https://www.scirp.org/journal/ojfd
ISSN Online: 2165-3860
ISSN Print: 2165-3852

Modeling of Coupled Heat and Mass Transfer in a Trapezoidal Porous Bed on a Grid

Kokou N'Wuitcha[1*], Gagnon Koffi Apedanou[2], Yendoubé Lare[2], Kossi Napo[2]

[1]Laboratoire sur l'Energie Solaire, Groupe Phénomènes de Transfert et Energétique (LES-GPTE), Faculté des Sciences, Université de Lomé, Lomé, Togo
[2]Laboratoire sur l'Energie Solaire, Chair Unesco, Faculté des Sciences, Université de Lomé, Lomé, Togo
Email: *knwuitcha@gmail.com

How to cite this paper: N'Wuitcha, K., Apedanou, G.K., Lare, Y. and Napo, K. (2023) Modeling of Coupled Heat and Mass Transfer in A Trapezoidal Porous Bed on A Grid. *Open Journal of Fluid Dynamics*, **13**, 1-15.
https://doi.org/10.4236/ojfd.2023.131001

Received: November 23, 2022
Accepted: February 12, 2023
Published: February 15, 2023

Abstract

We investigate heat and mass transfer in an isosceles trapezoidal cavity, filled with charcoal considered as a granular porous medium. The Darcy-Brinkman-Forchheimer flow model is coupled to the energy and mass equations with the assumption of non-thermal equilibrium. These equations are discretized by the finite volume method with an offset mesh and then solved by the line-by-line method of Thomas. The coupling between pressure and velocity is obtained by Semi-Implicit Method for Pressure Linked Equations (SIMPLE) algorithm. The results show that the temperature in the cavity increases when the inclination angle of the sides walls decreases. The 15˚ inclination is selected as being able to offer better thermal performance in the cookstove combustion chamber.

Keywords

Heat and Mass Transfer, Isosceles Trapezoidal Cavity, Porous Medium, Finite Volume Method, SIMPLE Algorithm

1. Introduction

Flow and heat transfer in porous media have been extensively studied numerically and experimentally because of their important applications. Flow in porous media is involved in various energy and environmental issues. We can mention, in a non-exhaustive way, the geological storage of gas (CO_2, natural, H_2), the management of nuclear and household waste, petroleum engineering, the combustion or drying of wood or the production of geothermal energy. However, the simulation of heat and mass transfer of coupled phenomena requires much larger computational resources. Nowadays, very powerful resources exist to effi-

ciently analyze and understand a complex set of heat and mass transfer problems. Recently, Narang *et al.* [1] demonstrated that the GPU (Graphical Processing Unit) can be much faster than the CPU (Compute Processing Unit) in the area of numerical heat and mass transfer solutions. Furthermore, the experimental results obtained for a radially composite capillary porous cylinder indicate that the GPU-based implementation shows a significant performance improvement over the CPU-based implementation with maximum speedups of about 10 times. AL-Amiri *et al.* [2] have made a numerical study presenting the laminar transport processes in a square cavity fed by a lid and filled with a water-saturated porous medium. A stable thermal stratification configuration is considered by imposing a vertical temperature gradient. The general formulation of the momentum equation is used such that inertial and viscous effects are incorporated. The relevant momentum and energy characteristics of the porous system are identified, with particular attention given to the implications of inertial effects. The Grashof number in this study was set to 104. A correlation of the Nusselt number is established based on the numerical results in the parametric domain. The results imply that inertial effects delay momentum and energy transport. However, these effects are more pronounced in the case of flow behaviour, which makes the computation more difficult. Increasing the Darcy number was found to induce an increase in the flow velocity and an increase in the fraction of energy transport by convection. Double diffusive mixed convection in a porous rectangular cavity saturated with a fluid is studied numerically by Khanafer and Vafai [3]. The two horizontal walls are fixed and maintained at different temperatures and concentrations. On the other hand, the two vertical walls are adiabatic and move with a constant velocity. The finite volume method is used to discretize the transport equations. The results indicate that the Darcy number, Lewis number and Richardson number have a great effect on the heat and mass transfer.

The influence of form factor on natural convection in a porous cavity with partially active vertical walls was examined by Bhuvaneswari *et al.* [4]. The mathematical model of the equations is the Darcy-Brinkman-Forchheimer model. Several heating or cooling positions are considered. The structure of the flow is found to be strongly influenced by the heating or cooling position as well as the heat transfer rate. Furthermore, they found that the rate of transfer decreases with increasing form factor. Basak *et al.* [5] performed finite element simulations to study the influence of uniform heating of the bottom wall of a trapezoidal enclosure at different tilt angles. The influence of Rayleigh number, Prandtl number and Darcy number was explored. The numerical results show heat transfer mainly due to conduction at low values of Darcy number. The flow intensity increases with increasing Darcy number. An increase in flow intensity and a larger temperature gradient are also observed with increasing the tilt angles from 0˚ to 45˚, especially for large values of Prandtl and Rayleigh. Bera *et al.* [6] investigated the natural double diffusion convection in a porous cavity outside of local

thermal equilibrium by the general Darcy-Brinkman-Forchheimer model and the finite volume method. The authors observed that at low values of the conductivity ratio, the increase of the interphase exchange coefficient leads to a decrease of the mean Nusselt of the fluid and an increase of that of the solid. Nevertheless, for a high conductivity ratio, the heat exchange in both phases is invariant to the exchange coefficient. Bourouis *et al.* [7] [8] presented two numerical studies of heat transfer by natural convection inside a porous cavity under the assumption of local thermal non-equilibrium. The flow is initiated by partial heating of the two vertical walls to constant temperatures; the other two horizontal walls are insulated. This flow is governed by the Darcy-Brinkman-Forchheimer model. The effect of cavity tilt angle, local thermal non-equilibrium parameters, Rayleigh number and Darcy number has been explored. The cavity tilt angle was found to have a significant influence on the transfer rate and on the difference between the two mean Nusselt numbers of the fluid and the solid. The mean Nusselt numbers of the fluid and solid increase with increasing Rayleigh and Darcy numbers. At low values of local thermal non-equilibrium parameters, the thermal equilibrium between the two phases is valid, however by increasing the Rayleigh and Darcy number, the thermal non-equilibrium model is found to be more accurate. B. Fersadou, and H. Kahalerras [9] treated mixed convection in a completely porous and differentially heated vertical channel. The Darcy-Brinkman-Forchheimer model with the Boussinesq approximation is adopted and the governing equations are solved by the finite volume method. The effect of the buoyancy force given by the Richardson, on the velocity and temperature fields is examined. The main results show an increase in the rate of heat transfer with decreasing Darcy number and an increasing Richardson number. W. Foudhil *et al.* [10] investigated the convective heat transfer in a vertical porous channel heated on one side and insulated on the other. The porous medium is formed by a solid matrix of spherical balls. The fluid considered is air which saturates the solid matrix. The two-temperature model and the Darcy-Brinkman-Forchheimer equation are adopted to represent this system and the porosity is considered as a space variable in the domain. The numerical model has been used to analyze the effect of several operating parameters on the heat transfer enhancement. The results show that the heat transfer decreases with the increase of the form factor. When the Biot number increases, the heat transfer between the walls and the porous domain increases. The heat transfer increases with the Reynolds number and with the thermal conductivity of the solid matrix. An increase in channel diameter induces a decrease in heat transfer. Correlations between the Nusselt number based on the particle diameter, the Reynolds number and the particle diameter have been established. In addition, the simulation results have been validated experimentally. Ahusborde *et al.* [11] modelled multiphase flows in reactive porous media by mass conservation laws for each chemical component and in each phase. The mass conservation laws are coupled to an energy conservation equation. Chemical reactions are represented by reaction rates which are either concentration dependent in the case of kinetic reac-

tions or unknown for equilibrium reactions. Kinetic reactions are modeled in the form of ordinary differential equations. This coupled system is solved by implementing an implicit finite volume method. The temporal discretization is performed using a backward scheme while the spatial discretization is based on a cell-centered method. The global solution of the problem is written as a nonlinear system which is solved using a Newtonian method with an adaptive time step. In our previous work [12], we gave necessary recommendations for the design of the primary air draft zone of the ASUTO improved charcoal cookstove to ensure better primary air draft to its combustion chamber in free convection. This paper focuses on the modeling of the fuel bed in the combustion chamber of the ASUTO charcoal cookstove. The heat and mass transfer phenomena in the charcoal bed considered as a porous medium filling a trapezoidal cavity on a grid saturated with a mixture of air and water vapor are studied. From this literature review, we deduce the following conclusions:

- The Darcy-Brinkman-Forchheimer model is the most general and best suited flow model for modeling combustion in porous media.
- The assumption of local thermal non-equilibrium between the phases or the two-temperature model would be suitable for the future consideration of charcoal combustion.
- The study of mixed convection in an isosceles trapezoidal cavity filled with a porous fixed bed on a grid has not been studied by researchers to our knowledge. This study is therefore a new development.

2. Physical Model

The problem considered in this paper concerns an isosceles trapezoidal cavity brought to a hot temperature on its inclined walls at an angle beta (β) to the vertical. The lower base, having the smallest diameter consists of a grid with six inlets of identical opening diameter between which adiabatic and equidistant walls are interposed. The upper base is open. This cavity is filled with a granular porous medium representing the charcoal bed in the combustion chamber of the ASUTO improved cookstove. Consider an air flow in this cavity; with heat and moisture transfer. The physical model of the problem is shown in **Figure 1** where the arrows represent the primary air inlet into the combustion chamber.

3. Mathematical Formulation

3.1. Simplifying Assumptions

The mixed convection flow in the charcoal-filled geometry of **Figure 1** is considered as a porous medium with the following assumptions:

- The flow is incompressible, viscous and laminar;
- Moist air is considered a Newtonian fluid;
- Thermophysical properties (other than density ρ) are assumed to be constant;
- Viscous dissipation is neglected in the energy equation;

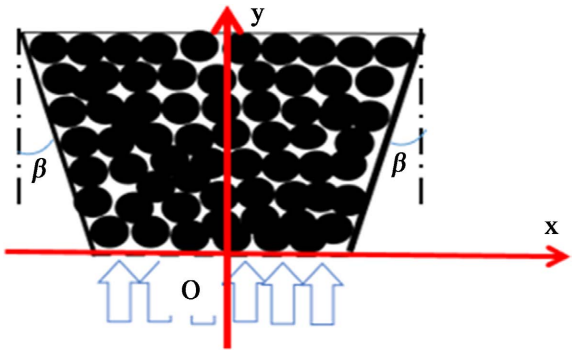

Figure 1. Physical model of the ASUTO's combustion chamber.

- The Boussinesq approximation is adopted;

3.2. Heat Transfer Equations

The equations of fluid motion with heat and mass transfer in the porous medium are:

Continuity equation

$$\frac{\partial u}{\partial x}+\frac{\partial v}{\partial y}=0 \tag{1}$$

Equation of motion of the fluid along (Ox)

$$\begin{aligned}&\frac{1}{\varepsilon}\frac{\partial u}{\partial t}+\frac{1}{\varepsilon^2}\left(\frac{\partial uu}{\partial x}+\frac{\partial uv}{\partial y}\right)\\&=-\frac{\partial p}{\partial x}+\frac{\mu_f}{\varepsilon}\left[\frac{\partial}{\partial x}\left(\frac{\partial u}{\partial x}\right)+\frac{\partial}{\partial y}\left(\frac{\partial u}{\partial y}\right)\right]-\left(\frac{\mu_f}{K}+\frac{\rho_f F\varepsilon}{\sqrt{K}}\left|\vec{W}\right|\right)u\end{aligned} \tag{2}$$

Equation of motion of the fluid along (Oy)

$$\begin{aligned}&\frac{1}{\varepsilon}\frac{\partial v}{\partial t}+\frac{1}{\varepsilon^2}\left(\frac{\partial uv}{\partial x}+\frac{\partial vv}{\partial y}\right)\\&=-\frac{\partial p}{\partial y}+\frac{\mu_f}{\varepsilon}\left[\frac{\partial}{\partial x}\left(\frac{\partial v}{\partial x}\right)+\frac{\partial}{\partial y}\left(\frac{\partial v}{\partial y}\right)\right]+\rho_f g-\left(\frac{\mu_f}{K}+\frac{\rho_f F\varepsilon}{\sqrt{K}}\left|\vec{W}\right|\right)v\end{aligned} \tag{3}$$

with $\left|\vec{W}\right|=\sqrt{u^2+v^2}$, u and v are the transverse and longitudinal components of the velocity, g Gravity field (m·s^{-2}).

- *Heat equation of the fluid phase*

$$\begin{aligned}&\varepsilon\left(\rho C_p\right)_f\frac{\partial}{\partial t}\left(T_f\right)+\left(\rho C_p\right)_f\frac{\partial}{\partial x}\left(uT_f\right)+\left(\rho C_p\right)_f\frac{\partial}{\partial y}\left(vT_f\right)\\&=\varepsilon\lambda_f\left[\frac{\partial}{\partial x}\left(\frac{\partial T_f}{\partial x}\right)+\frac{\partial}{\partial y}\left(\frac{\partial T_f}{\partial y}\right)\right]+h_{fs}a_{fs}\left(T_S-T_f\right)\end{aligned} \tag{4}$$

- *Heat equation of the solid phase*

$$\begin{aligned}&\left(1-\varepsilon\right)\left(\rho C_p\right)_s\frac{\partial}{\partial t}\left(T_S\right)\\&=\left(1-\varepsilon\right)\lambda_S\left[\frac{\partial}{\partial x}\left(\frac{\partial T_S}{\partial x}\right)+\frac{\partial}{\partial y}\left(\frac{\partial T_S}{\partial y}\right)\right]+h_{fs}a_{fs}\left(T_f-T_s\right)\end{aligned} \tag{5}$$

- *Moisture diffusion equation*

$$\varepsilon\frac{\partial}{\partial t}\left(Y_K\right)+\frac{\partial}{\partial x}\left(uY_K\right)+\frac{\partial}{\partial y}\left(vY_K\right)=D_K\left[\frac{\partial}{\partial x}\left(\frac{\partial Y_K}{\partial x}\right)+\frac{\partial}{\partial y}\left(\frac{\partial Y_K}{\partial y}\right)\right] \tag{6}$$

where

$K=\dfrac{d^2\varepsilon^3}{150\left(1-\varepsilon\right)^2}$, permeability of the porous medium (m^2)

$F=\dfrac{1.75}{\sqrt{150}\varepsilon^{1.5}}$, Forchheimer coefficient

$h_{fs}=\dfrac{\lambda f}{d}\left(2+1.1P_{rf}^{0.33}\left(\dfrac{vd}{\nu f}\right)^{0.6}\right)$, fluid-solid convective heat transfer coefficient ($W\cdot m^{-2}\cdot K^{-1}$)

$a_{fs}=\dfrac{6\left(1-\varepsilon\right)}{d}$, fluid-solid contact surface.

λ_f is the fluid Thermal conductivity ($W\cdot m^{-1}\cdot K^{-1}$), λ_s is the solid Thermal conductivity ($W\cdot m^{-1}\cdot K^{-1}$), H the Height (m), l the Smaller Base (m), L the high Base(m), T_f the fluid Temperature (K), T_s the solid Temperature(K), D the diffusion coefficient ($m^2\cdot s^{-1}$), Y_k the Mass titre, C_p Specific heat capacity ($J\cdot Kg^{-1}\cdot K^{-1}$)

3.3. Initial and Boundary Conditions

- Initial conditions

At the initial time,

$$u=v=0;\ T_f=T_S=T_0;\ Y_K=0;\ p=patm \tag{7}$$

- Boundary conditions:
- Grid or inlets

$$l_i\le x\le l_{i+1},\ i=2,4,6,8,10,12;$$

$$y=0;\ u=0;\ v=v_0;\ T_f=T_S=T_{amb};\ \text{et}\ Y_k=Y_k\ \text{initial} \tag{8}$$

- Inlets intermediates

$$l_i\le x\le l_{i+1},\ i=1,3,5,7,9,11,13;$$

$$y=0;\ u=v=0;\ \frac{\partial T_f}{\partial y}=0;\ \frac{\partial T_S}{\partial y}=0\ \text{et}\ Y_K=0 \tag{9}$$

- On the sides walls:

$$u=v=0;\ T_f=T_s=T_H;\ \frac{\partial Y_K}{\partial n}=0 \tag{10}$$

With n the outgoing normal of the side wall.

- On the upper horizontal wall

$$-\frac{L}{2}\le x\le+\frac{L}{2};\ y=H;\ \frac{\partial u}{\partial y}=\frac{\partial v}{\partial y}=0;\ \frac{\partial T_f}{\partial y}=\frac{\partial T_S}{\partial y}=0;\ \frac{\partial Y_K}{\partial y}=0 \tag{11}$$

4. Dimensionless Formulation of the Problem

The transfer equations associated with the initial and boundary conditions are

dimensioned by the following variables:

$$X=\frac{x}{H};\ Y=\frac{y}{H};\ U=\frac{u}{v_0};\ V=\frac{u}{v_0};\ \tau=\frac{v_0 t}{H};\ P=\frac{p-p_0}{\rho_e v_0^2} \tag{12}$$

4.1. Heat Transfer Equation

Introducing the variables of Equation (12) into Equations (1) to (6) leads to the following dimensionless equations:

- Continuity

$$\frac{\partial U}{\partial X}+\frac{\partial V}{\partial Y}=0 \tag{13}$$

- Equation of motion along (Ox)

$$\begin{aligned}&\varepsilon\frac{\partial U}{\partial \tau}+\frac{\partial UU}{\partial X}+\frac{\partial VU}{\partial Y}\\&=-\varepsilon^2\frac{\partial P}{\partial X}+\frac{\varepsilon r_{dL}}{R_{ep}}\left[\frac{\partial}{\partial X}\left(\frac{\partial U}{\partial X}\right)+\frac{\partial}{\partial Y}\left(\frac{\partial U}{\partial Y}\right)\right]\\&-\left(\frac{\varepsilon^2 r_{dL}}{R_{ep}Da}+\Lambda_L\varepsilon^2\sqrt{U^2+V^2}\right)U\end{aligned} \tag{14}$$

- Equation of motion following (Oy

$$\begin{aligned}&\varepsilon\frac{\partial V}{\partial \tau}+\frac{\partial UV}{\partial X}+\frac{\partial VV}{\partial Y}\\&=-\varepsilon^2\frac{\partial P}{\partial Y}+\frac{\varepsilon r_{dL}}{R_{ep}}\left[\frac{\partial}{\partial X}\left(\frac{\partial V}{\partial X}\right)+\frac{\partial}{\partial Y}\left(\frac{\partial V}{\partial Y}\right)\right]+\frac{G_{rf}\varepsilon^2 r_{dL}^2}{R_{ep}^2}\theta_f\\&-\left(\frac{\varepsilon^2 r_{dL}}{R_{ep}Da}+\Lambda_L\varepsilon^2\sqrt{U^2+V^2}\right)V\end{aligned} \tag{15}$$

- Heat equation of the fluid phase

$$\begin{aligned}&\varepsilon\frac{\partial}{\partial \tau}\left(\theta_f\right)+\frac{\partial}{\partial X}\left(U\theta_f\right)+\frac{\partial}{\partial Y}\left(V\theta_f\right)\\&=\frac{\varepsilon r_{dL}}{R_{ep}P_{rf}}\left[\frac{\partial}{\partial X}\left(\frac{\partial \theta_f}{\partial X}\right)+\frac{\partial}{\partial Y}\left(\frac{\partial \theta_f}{\partial Y}\right)\right]+\frac{r_{dL}B_i}{R_{ep}P_{rf}}\left(\theta_S-\theta_f\right)\end{aligned} \tag{16}$$

- Heat equation of the solid phase

$$(1-\varepsilon)\frac{\partial}{\partial \tau}\left(\theta_S\right)=\frac{(1-\varepsilon)r_{dL}}{R_{ep}P_{rf}}\left[\frac{\partial}{\partial X}\left(\frac{\partial \theta_S}{\partial X}\right)+\frac{\partial}{\partial Y}\left(\frac{\partial \theta_S}{\partial Y}\right)\right]+\frac{r_{dL}B_i}{R_{ep}P_{rf}}\left(\theta_f-\theta_S\right) \tag{17}$$

- Moisture diffusion equation

$$\varepsilon\frac{\partial}{\partial \tau}\left(Y_K\right)+\frac{\partial}{\partial X}\left(UY_K\right)+\frac{\partial}{\partial Y}\left(VY_K\right)=\frac{r_{dL}}{R_{ep}S_{ch}}\left[\frac{\partial}{\partial X}\left(\frac{\partial Y_K}{\partial X}\right)+\frac{\partial}{\partial Y}\left(\frac{\partial Y_K}{\partial Y}\right)\right] \tag{18}$$

The dimensionless numbers defined in Equations (14)-(18) are defined by $Da=\frac{K}{H^2}$; $\Lambda_H=F\frac{H}{\sqrt{K}}$; $B_i=\frac{h_{fs}a_{fs}H^2}{\lambda_f}$; $R_{ep}=V_0\frac{d}{\nu_f}$; $G_{rf}=\frac{g\beta(T_H-T_0)H^4}{\nu_f^2}$ and $r_{dL}=d/H$; $\lambda=\lambda_s/\lambda_f$ where $G_{rf}, P_{rf}, Da, \Lambda_H, R_{ep}$ and B_i are respec-

tively Grashoff number, Prandlt number, Darcy number, the inertia coefficient, Reynolds number, Biot number related to the fluid-solid exchanges. r_{dL} and λ are respectively the ratio between the diameter of the particles and the height of the channel and the ratio between the solid and fluid conductivities.

4.2. Initial Boundary Conditions

Initial conditions

$$U = V = 0;\ \theta_f = \theta_S = 0;\ Y_K = 0;\ P = 0 \tag{19}$$

Boundary conditions

- Grid or entries

$$l_i \le x \le l_{i+1},\ i = 2,4,6,8,10,12;$$

$$Y = 0;\ U = 0;\ V = 1;\ \theta_f = \theta_S = 0; \text{ et } Y_k = 1 \tag{20}$$

- Input intermediates

$$l_i \le x \le l_{i+1},\ i = 1,3,5,7,9,11,13;$$

$$Y = 0,\ U = V = 0,\ \frac{\partial \theta_f}{\partial Y} = 0,\ \frac{\partial \theta_S}{\partial Y} = 0 \text{ and } Y_K = 0 \tag{21}$$

- On the sidewalls:

$$U = V = 0,\ \theta_f = \theta_s = \frac{T_H - T_0}{\Delta T},\ \frac{\partial Y_K}{\partial n} = 0 \tag{22}$$

With n the outgoing normal of the sidewall.

- On the upper horizontal wall: Exit

$$-\frac{L}{2H} \le X \le \frac{L}{2H};\ Y = 1;\ \frac{\partial U}{\partial Y} = \frac{\partial V}{\partial Y} = 0;\ \frac{\partial \theta_f}{\partial Y} = \frac{\partial \theta_S}{\partial Y} = 0;\ \frac{\partial Y_K}{\partial Y} = 0 \tag{23}$$

5. Numerical Method

We discretize the above adimensional transfer equations and their associated initial and boundary conditions using the finite volume method. The matching between velocity and pressure fields is ensured by the SIMPLE (Semi-Implicit Method for Pressure-linked Equations) algorithm [13]. The systems of equations resulting from this discretization are solved using the THOMAS algorithm.

6. Validation

The qualitative and quantitative validation of our code has been performed against the work done by Foudhil *et al.* [10]. Thus, the local Nusselt number is calculated and compared with that of Foudhil *et al.* [10] in the case of a vertical flat-walled channel for a particle Reynolds number of 150 and 200 (**Figure 2**). We find a good qualitative and quantitative agreement because the relative error does not exceed 0.3%.

7. Results and Discussion

The objective of this part is to study the influences of the model's parameters like

the porosity of the bed, the Darcy number and the geometrical parameters like the inclination angle of the side walls on the flow structure, isotherms, temperature profiles and the moisture concentration.

7.1. Influence of the Bed Porosity

We present in Figure 3, the structure of the streamlines, the isotherms of the fluid and solid phase and the isovalues of the humidity for different value of the porosity ($\varepsilon = 0.5$; $\varepsilon = 0.6$; $\varepsilon = 0.8$). The overall structure of the streamlines is characterized by parallel lines springing from the grid at the bottom to the outlet at the top. The isotherms are overturned parabolas, symmetrical with respect to the

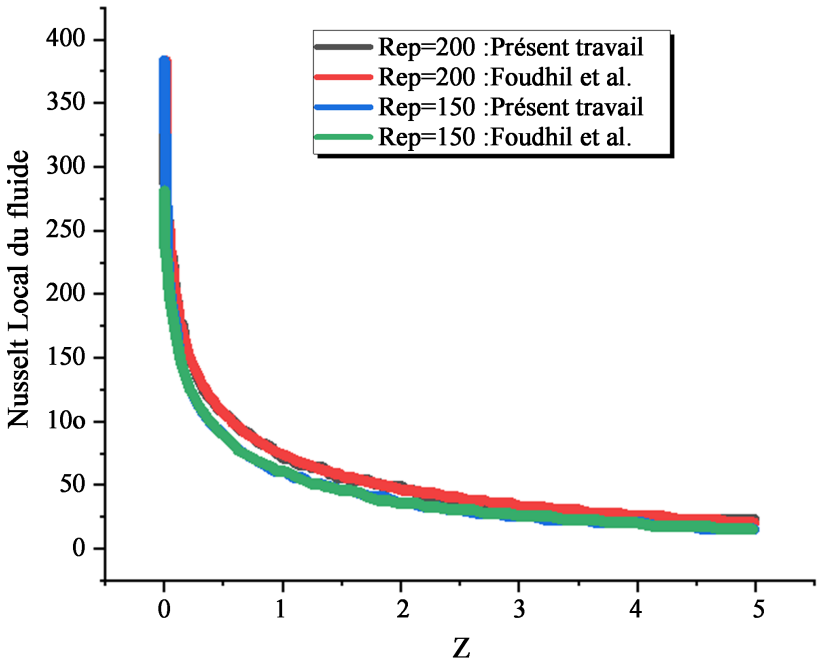

Figure 2. Comparaison of the fluid local Nusselt number.

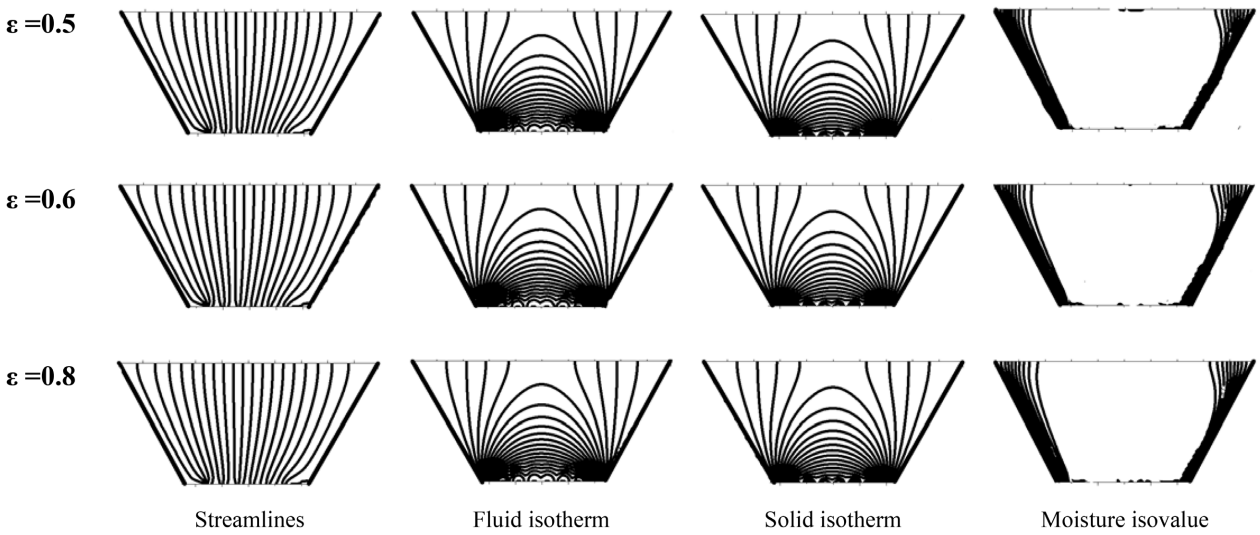

Figure 3. Influence of the bed porosity.

median of the bases of the trapezoidal cavity. The humidity isovalues show a uniformity inside the cavity with some variations at the near heated inclined walls. The structure of the streamline, isotherms and moisture do not show any significant variation with respect to the variation of the bed porosity. This result is confirmed by the temperature profiles presented in Figure 4 where we note a perfect agreement between the temperatures profiles in the cavity for the different values of porosity listed above. The variation of the bed porosity does not influence the streamlines, nor the isotherms or isovals of the humidity and temperature profiles in the cavity.

7.2. Influence of the Darcy Number

Figure 5 shows the streamlines, isotherms and moisture isovalues for different

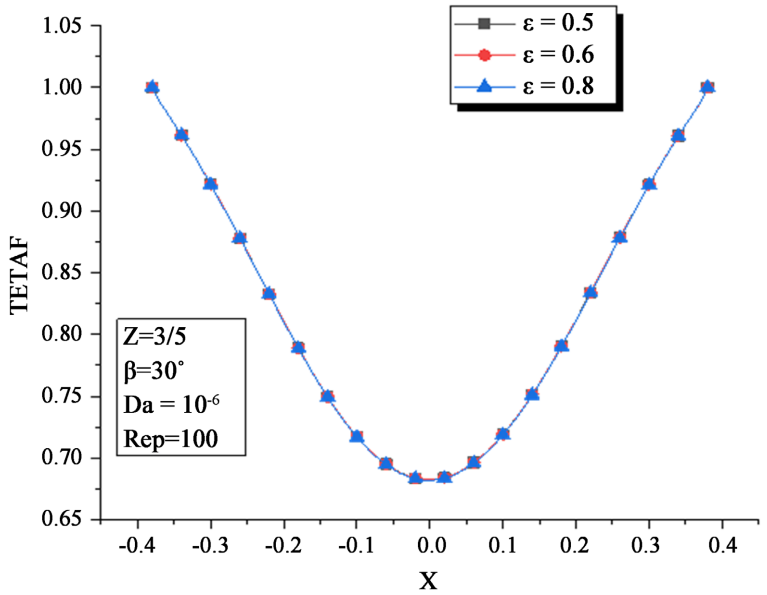

Figure 4. Influence of the porosity on the temperature profile.

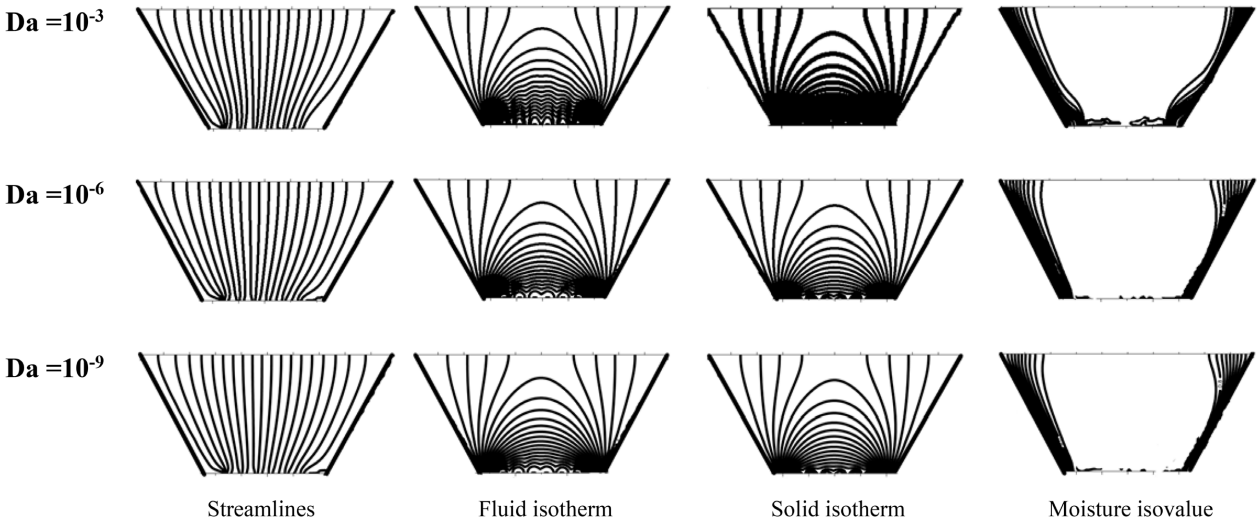

Figure 5. Influence of the Darcy number Da.

values of the Darcy number ($Da = 10^{-3}$; $Da = 10^{-6}$ and $Da = 10^{-9}$). The flow structure doesn't present a significant variation with respect to the variation of the Darcy number qualitatively. This same result is observed on the isotherms and moisture isovalues. Thus, in Figure 6 we observe quantitatively an agreement between the temperatures profiles in the cavity for the different values of the Darcy number. The temperature of the bed is not influenced by the variation of the Darcy number.

7.3. Influence of the Angle of Inclination of the Sides Walls

We presented on the Figure 7, the streamlines, isotherms and moisture isovalues

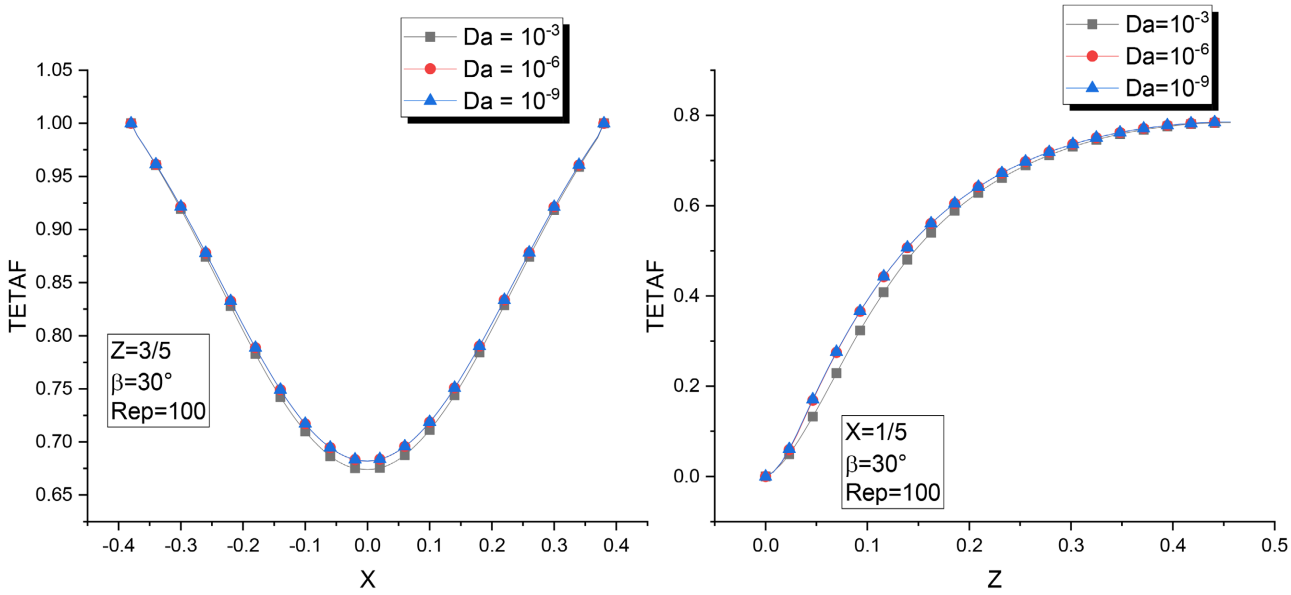

Figure 6. Influence of the Darcy number on the temperature profiles.

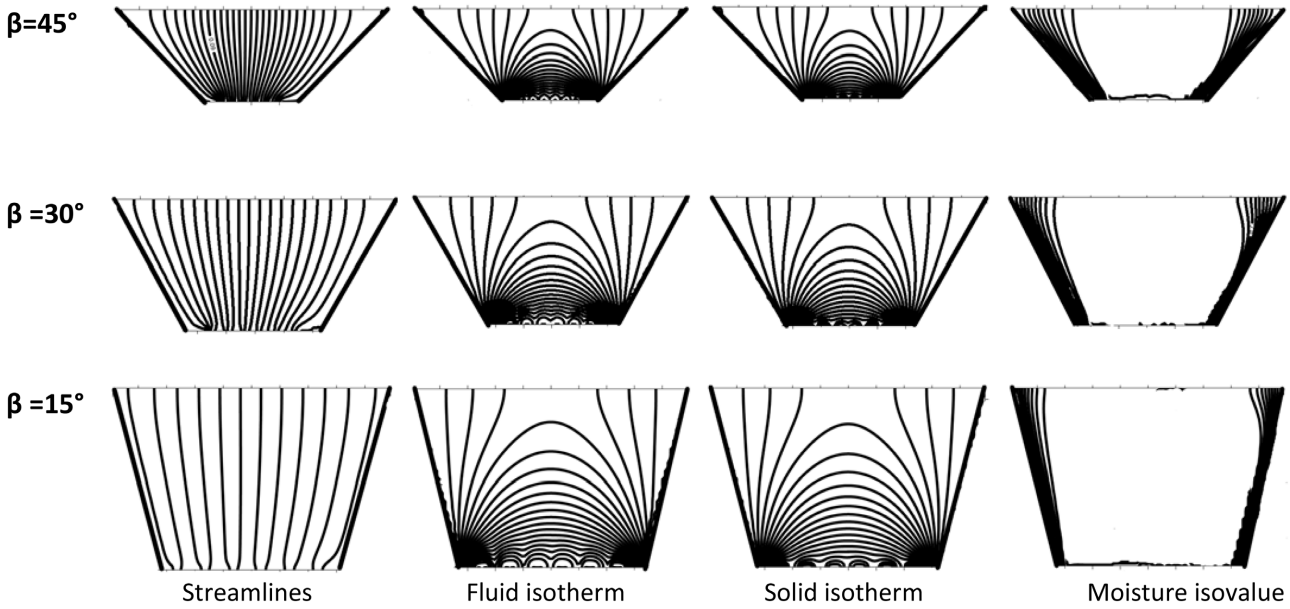

Figure 7. Influence of wall inclination.

for different inclinations of the combustion chamber sides walls.We notice no difference between the structure of the streamlines, the isotherms and the moisture isovalues in the cavity qualitatively. However, on Figure 8, presenting the temperature profiles, we notice an increase of the temperatures in the bed when the inclination angle of the sides walls decreases. The inclination of the wall of 15˚ with respect to the vertical offers a better thermal performance in the combustion chamber of the cookstove than the inclination angle 45˚.

7.4. Applicability of the Two-Temperature Model in Our Study

Figure 9 compares the temperature profiles of the fluid phase to that of the solid phase. Whether it is the temperature variation along the x-axis or y-axis, there is a discrepancy between the two profiles. This shows the validity of the two-temperature model in our study. Figure 10(a) shows the longitudinal velocity profile across the fuel bed while the pressure profile is shown in Figure 10(b). It shows a

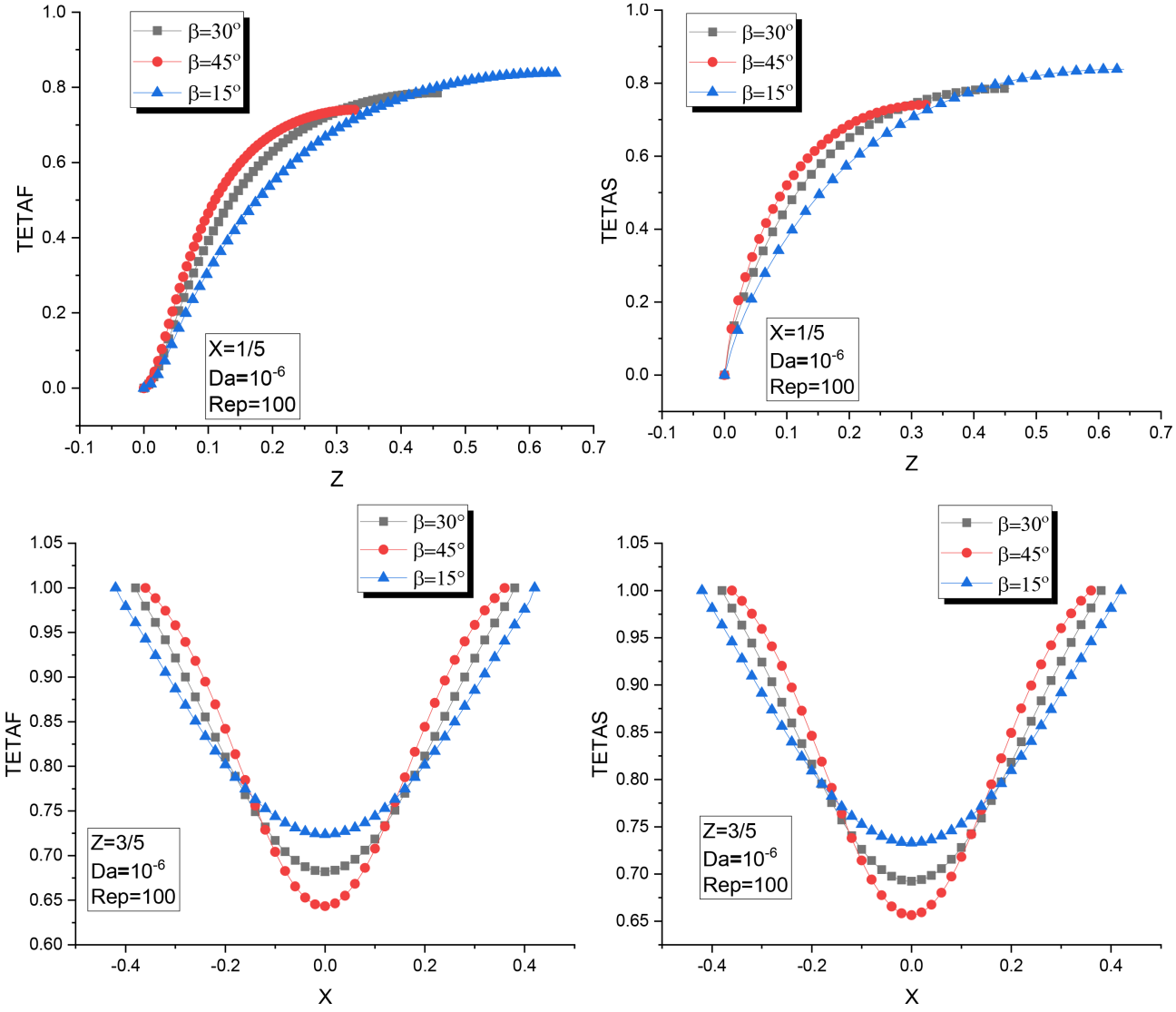

Figure 8. Influence of wall inclination on temperature profiles in the bed.

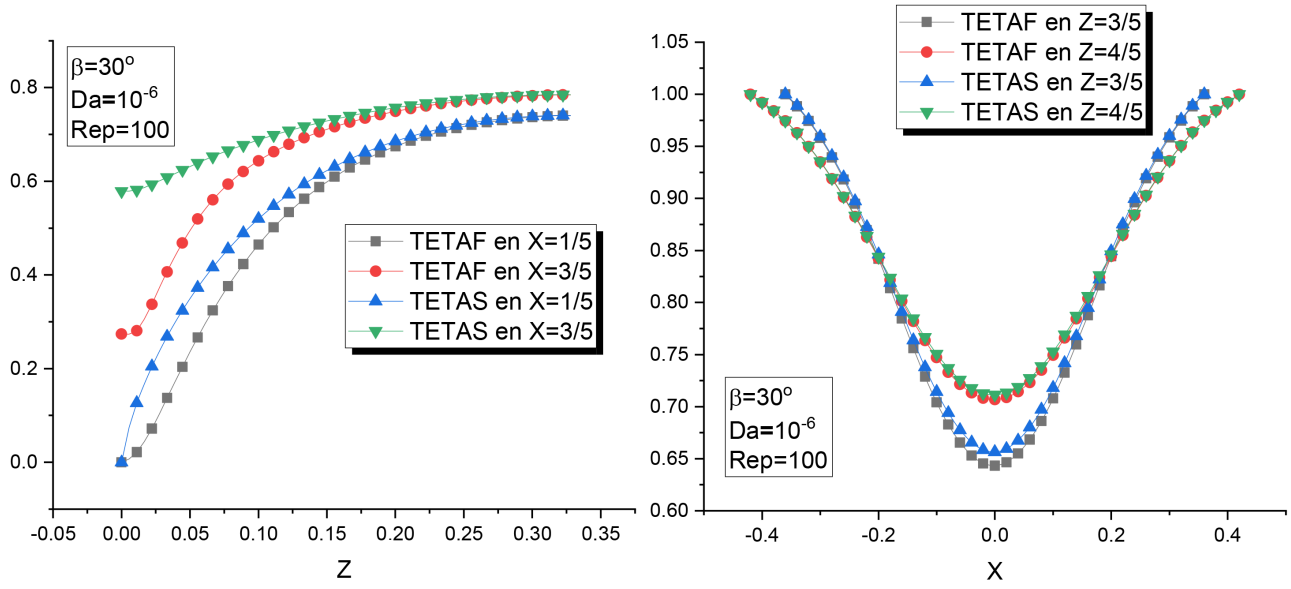

Figure 9. Applicability of the non-thermal equilibrium assumption.

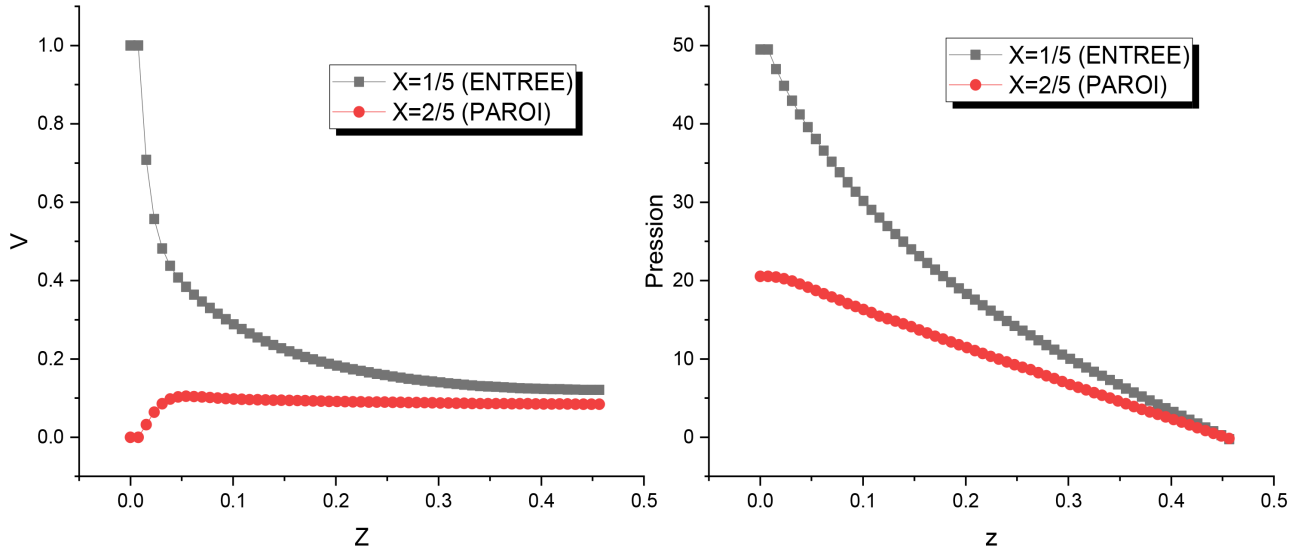

Figure 10. Velocity and longitudinal pressure profiles in the bed.

depression in the bed along its height.

8. Conclusion

In this paper, we studied heat and mass transfer in an isosceles trapezoidal cavity, open at the top and having a six-entry grid at the base. This cavity is filled with charcoal considered as a granular porous medium. The general Darcy-Brinkman-Forchheimer flow model is coupled to the energy and mass equations with the assumption of non-thermal equilibrium to describe the physical phenomena taking place. These equations are discretized by the finite volume method with an offset mesh and then solved by the line-by-line method of Thomas. The coupling between pressure and velocity is obtained by the SIMPLE (Semi-

Implicit Method for Pressure Linked Equation) algorithm. Our results compared to those of Foudhil *et al.* [10] show a good agreement. The sensitivity study carried out for results of two hours of simulation does not reveal any influence of the bed porosity as well as of the Darcy number on the bed temperature, which is an important parameter in our study, especially for the combustion chamber. On the other hand, the inclination of the walls turns out to be a controlling factor for the maximum temperature towards the cookstove outlet. Thus the temperature in the cavity increases when the inclination angle of the sides walls decreases. The 15˚ inclination is selected as being able to offer better thermal performance in the cookstove combustion chamber.

Conflicts of Interest

The authors declare no conflicts of interest regarding the publication of this paper.

References

[1] Narang, H., Wu, F. and Mohammed, A. (2019) An Efficient Acceleration of Solving Heat and Mass Transfer Equations with the First Kind Boundary Conditions in Capillary Porous Radially Composite Cylinder Using Programmable Graphics Hardware. *Journal of Computer and Communications*, **7**, 267-281. https://doi.org/10.4236/jcc.2019.77022

[2] Al-Amiri, A.M. (2000) Analysis of Momentum and Energy Transfer in a Lid-Driven Cavity Filled with a Porous Medium. *International Journal of Heat and Mass Transfer,* **43**, 3513-3527. https://doi.org/10.1016/S0017-9310(99)00391-9

[3] Khanafer, K. and Vafai, K. (2002) Double-Diffusive Mixed Convection in a Lid-Driven Enclosure Filled with a Fluid-Saturated Porous Medium. *Numerical Heat Transfer*, *Part A*: *Applications*, **42**, 465-486. https://doi.org/10.1080/10407780290059657

[4] Bhuvaneswari, M., Sivasankaran, S. and Kim, Y.J. (2011) Effect of Aspect Ratio on Convection in a Porous Enclosure with Partially Active Thermal Walls. *Computers & Mathematics with Applications*, **62**, 3844-3856. https://doi.org/10.1016/j.camwa.2011.09.033

[5] Basak, T., Roy, S., Singh, A. and Balakrishnan, A.R. (2009) Natural Convection Flows in Porous Trapezoidal Enclosures with Various Inclination Angles. *International Journal of Heat and Mass Transfer,* **52**, 4612-4623. https://doi.org/10.1016/j.ijheatmasstransfer.2009.01.050

[6] Bera, P., Pippal, S. and Sharma, A. (2014) A Thermal Non-Equilibrium Approach on Double-Diffusive Natural Convection in a Square Porous-Medium Cavity. *International Journal of Heat and Mass Transfer,* **78**, 1080-1094. https://doi.org/10.1016/j.ijheatmasstransfer.2014.07.041

[7] Bourouis, A., Omara, A. and Abboudi, S. (2015) Natural Convection in a Porous Cavity out of Local Thermal Equilibrium with Partially Active Walls. *XIIe Colloque Interuniversitaire Franco-Québécois sur la Thermique des Systèmes*, Sherbrooke, 8-10 Juin 2015.

[8] Bourouis, A., Omara, A. and Abboudi, S. (2015) Influence of the Tilt Angle on the Heat Transfer by Natural Convection in a Porous Cavity out of Thermal Equilibrium. *17èmes Journées Internationales de Thermique* (*Proceedings on CD*), Marseille, 28-30 October 2015.

[9] Fersadou, B. and Kahalerras, H. (2015) MHD Mixed Convection in a Vertical Porous Channel. *International Journal of Aerospace and Mechanical Engineering*, **9**, 1908-1912.

[10] Foudhil, W., Dhifaoui, B., Jabrallah, S.B., Belghith, A. and Corriou, J.P. (2012) Numerical and Experimental Study of Convective Heat Transfer in a Vertical Porous Channel Using a Non-Equilibrium Model. *Journal of Porous Media*, **15**, 531-547. https://doi.org/10.1615/JPorMedia.v15.i6.30

[11] Ahusborde, E., Croccolo, F. and Pillardou, N. (2022) Numerical Simulation of Thermo-Hydro-Chemical Processes for Subsurface Problems. *Sixteenth International Conference Zaragoza-Pau on Mathematics and Its Applications*, Jaca, 7-9 September 2022.

[12] Apedanou, G., N'wuitcha, K., Lare, Y. and Napo, K. (2022) Numerical Study of Mixed Convection in an Isosceles Trapezoidal Cavity with Several Outlets: Application for Primary Air Draft in ASUTO Charcoal Stove. *Modern Mechanical Engineering*, **12**, 45-61. https://doi.org/10.4236/mme.2022.122003

[13] Patankar, S. (1980) Numerical Heat Transfer and Fluid Flow. CRC Press, Boca Raton. https://doi.org/10.1201/9781482234213